Science
AAAS

Using ecological thresholds to evaluate the costs and benefits of set-asides in a biodiversity hotspot

Cristina Banks-Leite *et al.*

Science **345**, 1041 (2014);
DOI: 10.1126/science.1255768

Science (print ISSN 0036-8075; online ISSN 1095-9203) is published weekly, except the last week in December, by the American Association for the Advancement of Science, 1200 New York Avenue NW, Washington, DC 20005.

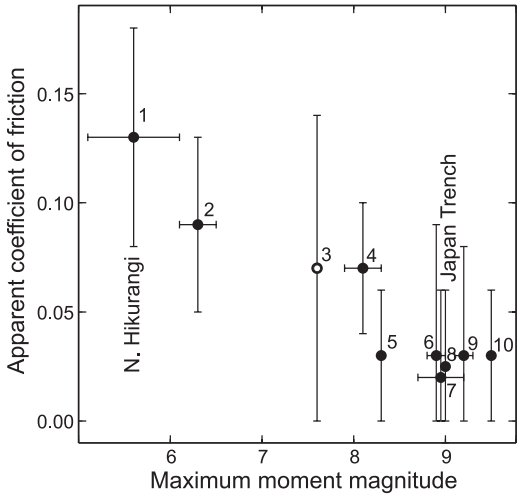

Fig. 4. Apparent friction of megathrust versus maximum size of clearly documented interplate earthquake. 1, northern Hikurangi; 2, Manila Trench; 3, Costa Rica; 4, Kermadec; 5, Nankai; 6, Kamchatka; 7, northern Cascadia; 8, Japan Trench; 9, Sumatra; and 10, south-central Chile (table S2). Except for Costa Rica (*11*), the apparent coefficients of friction are obtained using thermal models developed in this study, with error bars based on numerical testing of model fit to heat-flow data (Fig. 2 and figs. S1 to S7) (*11*). Error bars for M_{max} are based on publications on these earthquakes (table S2).

at each subduction zone (Fig. 4). The M_{max} values provide a proxy of long-term seismic slip. In determining M_{max} for northern Hikurangi, we do not consider two poorly recorded events in 1947 both with M_w ~ 7 (*29*), because they occurred at a very shallow depth of the plate interface and do not represent the general slip mode of the megathrust. For subduction zones with M_{max} 8.3 to 9.5, the fault motion is primarily stick-slip. Coseismic slip in their largest earthquakes is comparable to slip deficits accumulated over typical interseismic intervals of several hundred years, and geodetic observations show a high degree of megathrust locking at present (table S2). For three of the other four subduction zones, the present locking/creeping state of the megathrust is constrained by modern geodetic measurements (table S2). They show large creep, with northern Hikurangi having the most active creep (Fig. 1B). At Kermadec, the present creeping/locking state of the megathrust cannot be adequately determined by geodetic measurements (*30*). All the highly seismogenic subduction zones in this suite feature smooth subducting sea floor, and the faults are weaker than the faults associated with the subduction of rugged sea floor. The general correlation between subducting sea floor ruggedness, creeping, and greater heat dissipation suggests that geomorphological and thermal observations may be useful in assessing earthquake and tsunami hazards for risk mitigation.

REFERENCES AND NOTES

1. C. H. Scholz, J. Campos, *J. Geophys. Res.* **100** (B11), 22,103–22,105 (1995).
2. K. Wang, S. L. Bilek, *Tectonophys.* **610**, 1–24 (2014).
3. K. Wang, S. L. Bilek, *Geology* **39**, 819–822 (2011).
4. A. Heuret, C. P. Conrad, F. Funiciello, S. Lallemand, L. Sandri, *Geophys. Res. Lett.* **39**, L05304 (2012).
5. D. W. Scholl, S. H. Kirby, R. von Huene, American Geophysical Union Fall Meeting, Abstract T14B–01 (2011).
6. Y. Yamanaka, M. Kikuchi, *J. Geophys. Res.* **109**, B07307 (2004).
7. N. Uchida, T. Matsuzawa, *Earth Planets Space* **63**, 675–679 (2011).
8. T. Webb, H. Anderson, *Geophys. J. Int.* **134**, 40–86 (1998).
9. L. M. Wallace *et al.*, *Geochem. Geophys. Geosyst.* **10**, Q10006 (2009).
10. D. H. N. Barker, R. Sutherland, S. Henrys, S. Bannister, *Geochem. Geophys. Geosyst.* **10**, Q02007 (2009).
11. Materials, methods, and other information are available as supplementary material on *Science* Online.
12. C. A. J. Wibberley, G. Yielding, G. Di Toro, in *The Internal Structure of Fault Zones: Implications for Mechanical and Fluid-Flow Properties*, Geol. Soc. Lond. Spec. Pub. 299, C. A. J. Wibberley, W. Kurz, J. Imber, R. E. Holdsworth, C. Collettini, Eds. (Geological Society of London, 2008), pp. 5–33.
13. H. Kanamori, L. Rivera, in *The missing sinks: Slip localization in faults, damage zones, and the seismic energy budget*, Geophys. Monogr. 170, Abercrombie, R., Ed. (America Geophysical Union, Washington DC, 2006), pp. 3–13.
14. H. Noda, T. Shimamoto, *J. Struct. Geol.* **38**, 234–242 (2012).
15. J. Byerlee, *Pure Appl. Geophys.* **116**, 615–626 (1978).
16. K. Wang, K. Suyehiro, *Geophys. Res. Lett.* **26**, 2307–2310 (1999).
17. S. Lamb, *J. Geophys. Res.* **111**, B07401 (2006).
18. Y. Kawada, M. Yamano, N. Seama, *Geochem. Geophys. Geosyst.* **15**, 1580–1599 (2014).
19. G. Di Toro *et al.*, *Nature* **471**, 494–498 (2011).
20. B. P. Allmann, P. M. Shearer, *J. Geophys. Res.* **114** (B1), B01310 (2009).
21. K. Koketsu *et al.*, *Earth Planet. Sci. Lett.* **310**, 480–487 (2011).
22. S. J. Lee, B. S. Huang, M. Ando, H. C. Chiu, J. H. Wang, *Geophys. Res. Lett.* **38**, L19306 (2011).
23. H. Kumagai, N. Pulido, E. Fukuyama, S. Aoi, *Earth Planets Space* **64**, 649–654 (2012).
24. In some earthquakes, the final fault stress at the end of the rupture may be somewhat smaller (overshoot) or larger (undershoot) than the fault strength during slip, but the deviation from the coseismic strength is expected to be a small fraction of the stress drop.
25. A. Hasegawa *et al.*, *Earth Planet. Sci. Lett.* **355-356**, 231–243 (2012).
26. M. E. Pritchard, M. Simons, *J. Geophys. Res.* **111**, B08405 (2006).
27. R. E. Abercrombie, J. R. Rice, *Geophys. J. Int.* **162**, 406–424 (2005).
28. D. A. Lockner, C. Morrow, D. Moore, S. Hickman, *Nature* **472**, 82–85 (2011).
29. D. I. Doser, T. H. Webb, *Geophys. J. Int.* **152**, 795–832 (2003).
30. W. Power, L. Wallace, X. Wang, M. Reyners, *Pure Appl. Geophys.* **169**, 1–36 (2012).

ACKNOWLEDGMENTS

We thank J. He for writing finite element code PGCTherm and implementing the line-element method for fault modeling, W. -C. Chi for making available digital heat-flow data for Manila Trench, and S. Wu and J. Zhang for discussions. X.G. was supported by Chinese Academy of Sciences' Strategic Priority Research Program Grant XDA11030102 and Open Foundation of Key Laboratory of Marine Geology and Environment Grant MGE2012KG04, and K.W. was supported by Geological Survey of Canada core funding and a Natural Sciences and Engineering Research Council of Canada Discovery Grant through the University of Victoria. This is Geological Survey of Canada contribution 2014105. All heat-flow data used are from published sources as listed in the reference list. Modeling parameters and tabulated results are available in the supplementary materials.

SUPPLEMENTARY MATERIALS

www.sciencemag.org/content/345/6200/1038/suppl/DC1
Materials and Methods
Supplementary Text
Figs. S1 to S7
Tables S1 and S2
References (*31*–*109*)

1 May 2014; accepted 18 July 2014
10.1126/science.1255487

CONSERVATION ECONOMICS

Using ecological thresholds to evaluate the costs and benefits of set-asides in a biodiversity hotspot

Cristina Banks-Leite,[1,2]* Renata Pardini,[3] Leandro R. Tambosi,[2] William D. Pearse,[4] Adriana A. Bueno,[5] Roberta T. Bruscagin,[2] Thais H. Condez,[6] Marianna Dixo,[2] Alexandre T. Igari,[7] Alexandre C. Martensen,[8] Jean Paul Metzger[2]

Ecological set-asides are a promising strategy for conserving biodiversity in human-modified landscapes; however, landowner participation is often precluded by financial constraints. We assessed the ecological benefits and economic costs of paying landowners to set aside private land for restoration. Benefits were calculated from data on nearly 25,000 captures of Brazilian Atlantic Forest vertebrates, and economic costs were estimated for several restoration scenarios and values of payment for ecosystem services. We show that an annual investment equivalent to 6.5% of what Brazil spends on agricultural subsidies would revert species composition and ecological functions across farmlands to levels found inside protected areas, thereby benefiting local people. Hence, efforts to secure the future of this and other biodiversity hotspots may be cost-effective.

The combined effects of environmental change are driving species to the brink of extinction across the world's biodiversity hotspots (*1*). If species disappear, the ecological functions they perform will also decline (*2*), with potential consequences including increased pest outbreaks and reduced food security (*3*, *4*). Although the role of large protected areas in preserving species is unquestionable (*5*), people will benefit more widely from

the ecological functions they perform if species occur throughout the biome, not just inside protected areas (*6*). It is in this context that ecological set-asides on private land have emerged as a promising strategy to preserve species and ecological functions across farmlands (*2*, *7*).

Setting aside private land for conservation nonetheless comes with financial costs to the landowner. For instance, in the Atlantic Forest of Brazil, the median yearly gross profit per hectare of agricultural land is $467 (interquartile range $199 to $868; U.S. dollars) (*8*), which is more than the Brazilian minimum wage. Conservation schemes that involve payment for ecosystem services (PES) provide a mechanism to increase landowner participation on set-asides (*9*), and its feasibility is reflected in the ever-increasing number of PES projects across the globe (*7*, *10*). However, most PES projects involving set-asides are relatively local initiatives that do not match the extensive scale of conservation needs and societal issues observed across biodiversity hotspots (*10*). Because large-scale problems require large-scale solutions, we here advocate and provide a realistic plan for a biome-wide set-aside program that concurrently maximizes the provision of habitat to biodiversity, and of ecological functions across rural areas, while minimizing the costs to society. Our aim is to calculate the overall economic costs of a set-aside program tailored to one of the most threatened hotspots of the world (*11*)—the Atlantic Forest of Brazil.

First, we estimated the minimum amount of habitat required to maintain biodiversity. This information is crucial (*12*); if too much area is set aside for conservation, economic costs become an impediment, but if not enough area is set aside, ecological gains are minor. To investigate the relationship between forest cover and species composition, we used data from a large field study conducted in the Atlantic Forest (*13*, *14*). The data set consisted of nearly 25,000 captures of 43 species of mammals, 140 species of birds, and 29 species of amphibians collected in 79 landscapes (200 ha each) varying from 5 to 100% of forest cover (including both old-growth and regrowth) and distributed across a 150-km-wide region (fig. S1) (*8*). For all groups, reduction in forest cover had a similar effect on community integrity, defined here as the similarity in community composition between fragmented and continuously forested landscapes (Fig. 1, I to L). Results indicate that community integrity of all three groups is maintained until 24 to 33% of forest cover, below which integrity declines sharply with further reductions in forest cover. When all three taxa were combined, analyses indicated the existence of a threshold at 28.5% of forest cover [95% confidence interval (CI) 24.0 to 33.1, $N = 56$], hence approximately 30% of native habitat is needed to preserve the integrity of vertebrate communities within each landscape (Fig. 1). Similar results have been observed previously in the northern Atlantic Forest, indicating that the patterns we discern are not exclusive to our sites, to vertebrates, or to a particular landscape scale (*8*, *15*).

Theoretical predictions have suggested that species become more sensitive to habitat alterations below 30% of remaining habitat (*16*). Our results, however, show that community responses are not solely restricted to species loss, as we observed a replacement of forest specialists by species adapted to disturbance (Fig. 1, A to D) (*8*, *17*). Forest specialists make up 75.9% of all species found in areas with 100% forest cover, whereas disturbance-adapted species represent 73% of species in landscapes with ≤10% forest cover (Fig. 1, A to D). Note that the threshold observed for community integrity is caused by a change in dominance; communities above the 30% cover threshold tend to be dominated (i.e., ≥50%) by forest specialists, and communities below the threshold become dominated by disturbance-adapted species (Fig. 1, E to H).

Although the causes and consequences of local species extinction are unknown, we found a strong correlation between species sensitivity and endemism (Pearson's $r = 0.87$, $N = 79$; fig. S2) (*8*), with 70.1% of forest specialists found to be endemic to the Atlantic Forest, whereas 68.5% of disturbance-adapted species occur in other biomes (Fig. 1, A to H). Previous studies have shown that forest specialists present narrow niche breadths and high efficiency in resource exploitation, so the loss of forest specialists potentially affects trophic cascades and ecological functions, such as seed dispersal and pest control (*18*–*20*). Detailed knowledge about the functional role of many Atlantic Forest vertebrates is not available (*8*), but if we assume niche conservatism (*21*), it is possible to infer that changes in lineage composition should broadly correspond to changes across functionally important traits (*22*). Hence, we estimated the phylogenetic integrity of communities, measured as the phylogenetic similarity or fraction of branch length shared between communities present in fragmented and continuously forested landscapes (*8*, *23*). We observed that phylogenetic integrity also decreases below the 30% cover threshold (Fig. 1, M to P), which suggests that the suite of ecological functions performed by these taxa are different above and below the threshold. Our findings highlight the importance of maintaining or restoring forest cover in the Atlantic Forest above the 30% threshold, as extinction of endemic species will lead to the loss of ecological functions that only these species provide.

Upscaling our results to 143 Mha of Atlantic Forest shows that although community integrity is high inside and around protected areas, it is much reduced across the 88.2% of the biome where less than 30% forest cover remains (using 200-ha landscape units; Fig. 2) (*8*). These results reinforce the need to preserve large existing remnants, as they provide a refuge to many species (*5*) (Figs. 1 and 2), and show that the Atlantic Forest is in urgent need of restoration to ensure that biodiversity-derived ecological functions are provided across the biome.

An area of 32.11 Mha would have to be restored to increase every 200-ha landscape of Atlantic Forest to a minimum of 30% forest cover. This is arguably an unfeasible goal, given the livelihoods and needs of 130 million Brazilians living in this biome. However, if we select landscapes with forest cover approaching the threshold, restoration in rural areas becomes better value for money (*8*). This is because highly deforested areas are typically depauperate of forest specialists (*13*, *15*, *24*), and the chances of recolonization after restoration would depend on money- and time-consuming interventions such as translocation. Thus, on the basis of our results and previous prioritization frameworks (*8*, *25*), we selected all landscapes with more than 20% forest cover and calculated how much area would be required to increase these target landscapes to 30% forest cover. Following this framework, we estimate that restoring just 424,000 ha across the biome will push forest cover to 30% in 37,000 landscapes, which together encompass a total area of 7.8 Mha (table S1). Restoring to 30% forest cover will provide benefits to biodiversity but is unlikely to provide a safety net, as it will bring communities just up to the threshold. Preferably, landscapes would be restored to a level of forest cover above the threshold, but this brings additional issues because the amount of area needed for restoration increases at an average rate of 114,000 ha (SE ±2300 ha) for every 1% increase in targeted forest cover (Fig. 3 and table S1) (*8*).

The Brazilian government and local NGOs have been steadily implementing PES schemes for set-asides on private land over the years (*10*). Taking the average PES values across the biome, $132.73 ha^{-1} per year (*10*), it would cost $56.3 million per year (range $25.7 million to $91.6 million; table S1) to target enough set-asides to reach the restoration target of 30% cover in the priority landscapes, and that cost would increase by $15.1 million (SE ±$300,000) per year for every 1% increase in targeted forest cover (table S1) (*8*). Although most areas would follow natural regeneration simply by ceasing the drivers of disturbance (*26*), it has been estimated that 20% of the area considered for restoration would require active reforestation practices, with associated costs of up to $5000/ha during the first 3 years (*26*). Thus, the overall budget to reach 30% forest cover in priority landscapes is $198 million per year, or 6.5% of Brazil's annual expenditure on agricultural subsidies for the first 3 years. This

[1]Grand Challenges in the Ecosystem and Environment, Department of Life Sciences, Imperial College London, Silwood Park Campus, Ascot SL5 7PY, UK. [2]Departamento de Ecologia, Instituto de Biociências, Universidade de São Paulo, 05508-090 São Paulo SP, Brazil. [3]Departamento de Zoologia, Instituto de Biociências, Universidade de São Paulo, 05508-090 São Paulo SP, Brazil. [4]Department of Ecology, Evolution, and Behavior, University of Minnesota, St. Paul, MN 55108, USA. [5]Fundação Florestal, Rua do Horto 931, 02377-000 São Paulo SP, Brazil. [6]Departamento de Zoologia, Instituto de Biociências, Universidade Estadual Paulista, 13506-900 Rio Claro SP, Brazil. [7]Curso de Gestão Ambiental, Escola de Artes, Ciências e Humanidades, Universidade de São Paulo, 03828-000 São Paulo SP, Brazil. [8]Department of Ecology and Evolutionary Biology, University of Toronto, Toronto, Ontario M5S 3B2, Canada.
***Corresponding author. E-mail: c.banks@imperial.ac.uk**

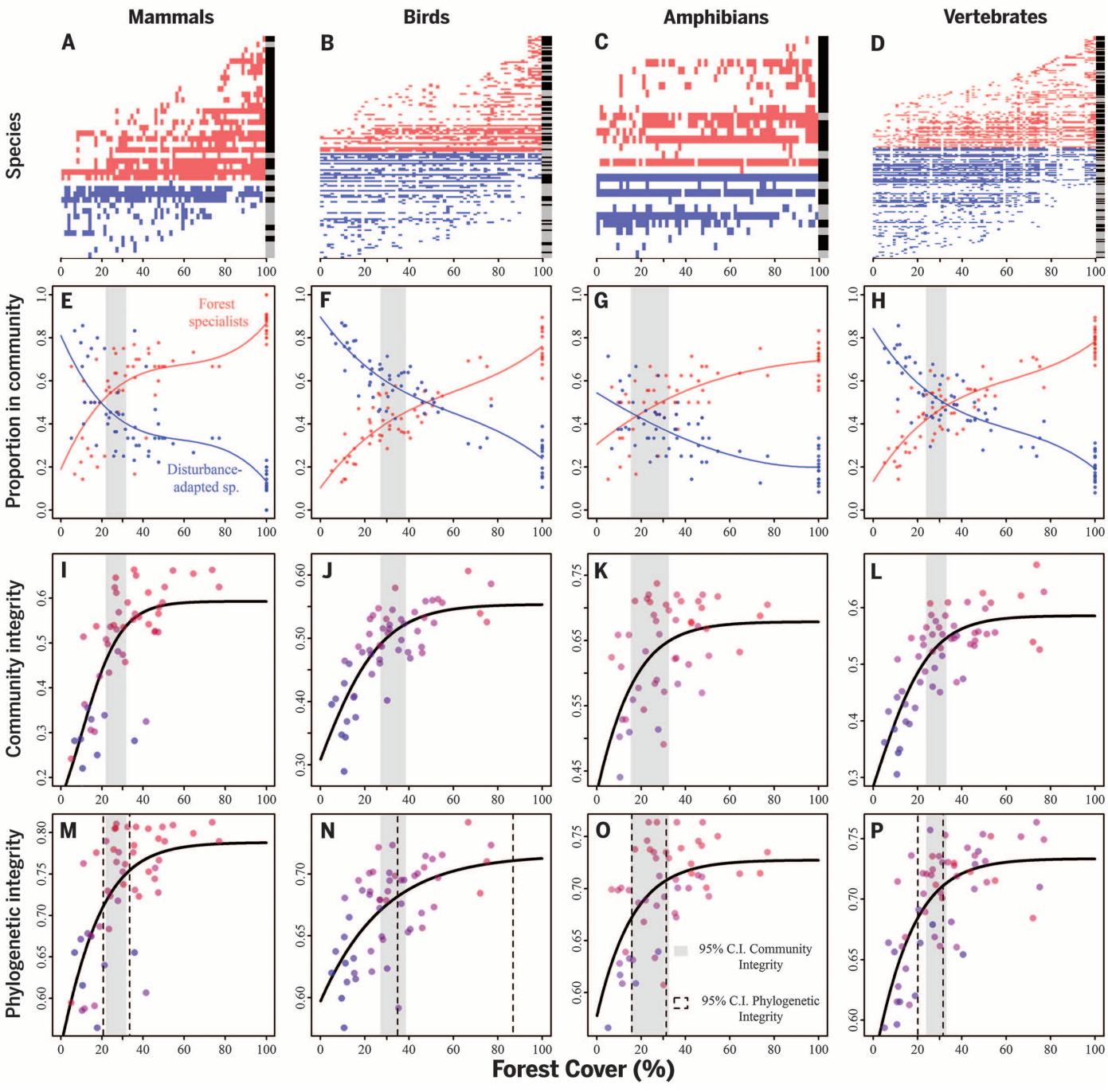

Fig. 1. Community and phylogenetic responses to forest cover in the Atlantic Forest. (**A** to **D**) Species × site matrix of mammals, birds, amphibians, and vertebrates. Sites (columns) are ordered by forest cover, and species (lines) are ordered by their preference to forest cover. Red indicates forest specialists; blue indicates disturbance-adapted species. Columns to the right of each panel represent endemism to the Atlantic Forest, with black cells showing endemic species and gray cells showing nonendemics. (**E** to **H**) Proportional change of forest specialists and disturbance-adapted species in each community. (**I** to **L**) Variation in community integrity. (**M** to **P**) Variation in phylogenetic integrity. Shaded areas in (E) to (P) indicate 95% CIs of threshold estimates obtained from community integrity. In (I) to (P), points are colored to represent the proportion of forest specialists and disturbance-adapted species. Area represented by two dashed lines in (M) to (P) indicates the CI of threshold obtained from phylogenetic integrity.

investment represents 0.0092% of Brazilian annual GDP, and the cost would reduce further to 0.0026% of Brazilian annual GDP once regeneration is under way (Fig. 3).

Creating set-asides to restore priority landscapes back to 30% forest cover may not save the most threatened species from extinction, but it would increase biodiversity and the ecological functions that species provide across rural areas (e.g., pest control and pollination) to a level similar to what is observed in protected areas (Figs. 1 and 3). Set-asides in priority landscapes would incur a loss of only 0.61% of the agricultural GDP produced in these municipalities (*8*), and payments would be targeted directly toward the very same people that would spare their land for conservation (*9*). Only rarely are the trade-offs between ecological gains and economic costs this

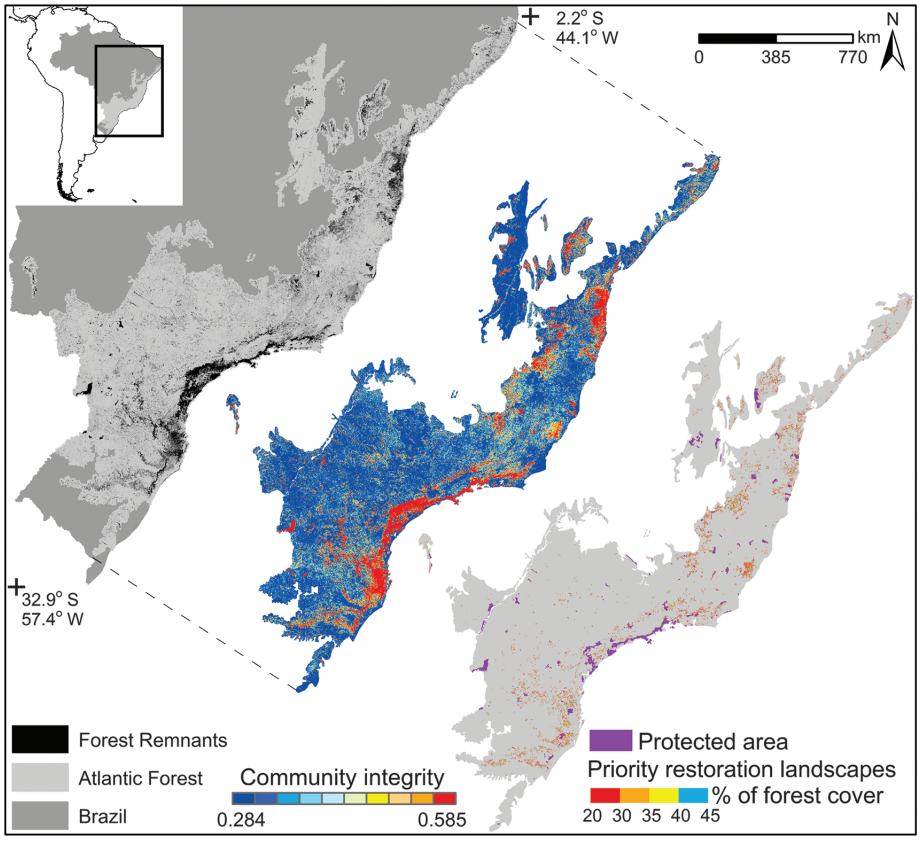

Fig. 2. Upscaling community integrity results for the Atlantic Forest of Brazil. From left to right, map of Atlantic Forest's historic distribution (gray) and current forest remnants (black), map of predicted community integrity of vertebrates across the biome, and map of priority areas for restoration (as well as current network of protected areas in purple). Large values (red) of community integrity indicate where communities have similar species composition relative to protected areas.

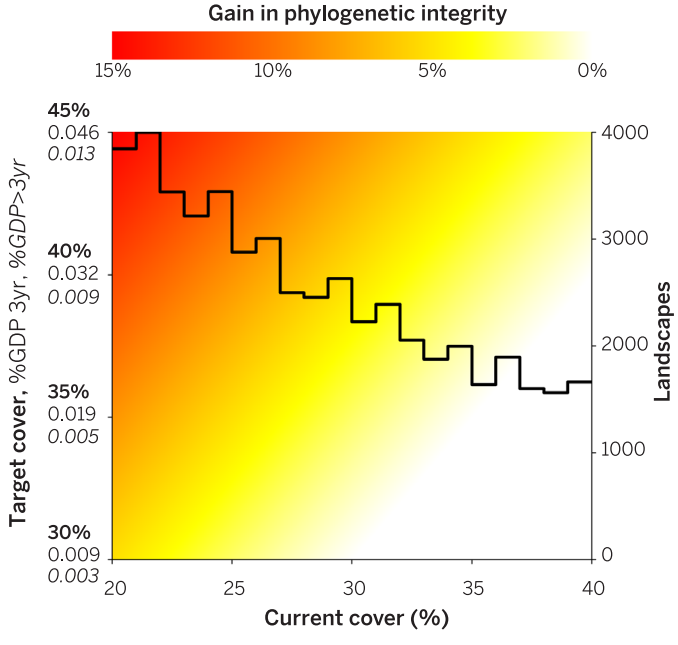

Fig. 3. Trade-offs in economic costs and ecological gains for a biome-wide set-aside program. Gains in phylogenetic integrity (measured as changes in PhyloSor index) are dependent on current percentage of forest cover and on amount of restoration targeted. Dark red indicates gains of up to 15% in phylogenetic integrity; white indicates decrease or no increase in integrity. Left *y* axis indicates target forest cover (in bold), costs relative to Brazil's GDP for the first 3 years (including PES and active restoration costs in priority landscapes), and costs for maintaining set-asides after the first 3 years (in italics). Black line depicts a histogram showing the number of existing priority landscapes in each class of forest cover.

simple; the costs relative to Brazil's GDP are low, those losing productive land are the ones that will directly benefit from PES, ecosystem services (e.g., air and soil quality, carbon storage) would be indirectly enhanced, and the ecosystem itself is one of the most charismatic in the world. At present, the Brazilian Atlantic Forest and other biodiversity hotspots are in serious danger of suffering large losses of endemic species. Our results show that this need not be the case.

REFERENCES AND NOTES

1. T. M. Brooks *et al.*, *Conserv. Biol.* **16**, 909–923 (2002).
2. A. Dobson *et al.*, *Ecology* **87**, 1915–1924 (2006).
3. J. E. Losey, M. Vaughan, *Bioscience* **56**, 311–323 (2006).
4. C. H. Sekercioğlu, G. C. Daily, P. R. Ehrlich, *Proc. Natl. Acad. Sci. U.S.A.* **101**, 18042–18047 (2004).
5. L. Naughton-Treves, M. B. Holland, K. Brandon, *Annu. Rev. Environ. Resour.* **30**, 219–252 (2005).
6. T. A. Gardner *et al.*, *Ecol. Lett.* **12**, 561–582 (2009).
7. J. Van Buskirk, Y. Willi, *Conserv. Biol.* **18**, 987–994 (2004).
8. See supplementary materials on *Science* Online.
9. J. Milder, S. Scherr, C. Bracer, *Ecol. Soc.* **15**, 4 (2010).
10. F. B. Guedes, S. E. Seehusen, *Pagamentos por Serviços Ambientais na Mata Atlântica: Lições aprendidas e desafios* (Ministério do Meio Ambiente, Brazil, 2011).
11. N. Myers, R. A. Mittermeier, C. G. Mittermeier, G. A. da Fonseca, J. Kent, *Nature* **403**, 853–858 (2000).
12. F. P. L. Melo, V. Arroyo-Rodríguez, L. Fahrig, M. Martínez-Ramos, M. Tabarelli, *Trends Ecol. Evol.* **28**, 462–468 (2013).
13. R. Pardini, A. A. Bueno, T. A. Gardner, P. I. Prado, J. P. Metzger, *PLOS ONE* **5**, e13666 (2010).
14. C. Banks-Leite, R. M. Ewers, V. Kapos, A. C. Martensen, J. P. Metzger, *J. Appl. Ecol.* **48**, 706–714 (2011).
15. M. M. Lima, E. Mariano-Neto, *For. Ecol. Manage.* **312**, 260–270 (2014).
16. H. Andren, *Oikos* **71**, 355–366 (1994).
17. C. Banks-Leite, R. M. Ewers, J. P. Metzger, *Ecology* **93**, 2560–2569 (2012).
18. D. L. Finke, W. E. Snyder, *Science* **321**, 1488–1490 (2008).
19. D. P. Edwards *et al.*, *Conserv. Biol.* **27**, 1079–1086 (2013).
20. M. Galetti *et al.*, *Science* **340**, 1086–1090 (2013).
21. J. J. Wiens *et al.*, *Ecol. Lett.* **13**, 1310–1324 (2010).
22. J. Cavender-Bares, K. H. Kozak, P. V. A. Fine, S. W. Kembel, *Ecol. Lett.* **12**, 693–715 (2009).
23. J. A. Bryant *et al.*, *Proc. Natl. Acad. Sci. U.S.A.* **105** (suppl. 1), 11505–11511 (2008).
24. A. C. Martensen, M. C. Ribeiro, C. Banks-Leite, P. I. Prado, J. P. Metzger, *Conserv. Biol.* **26**, 1100–1111 (2012).

25. L. R. Tambosi, A. C. Martensen, M. C. Ribeiro, J. P. Metzger, *Restor. Ecol.* **22**, 169–177 (2014).
26. F. P. L. Melo *et al.*, *Environ. Sci. Policy* **33**, 395–404 (2013).

ACKNOWLEDGMENTS

We thank R. Didham, T. Gardner, R. Gill, and R. Ewers for comments on the manuscript. Supported by NERC grant NE/H016228/1 (C.B.L.), CNPq research fellowship 306715/2011-2 (R.P.), FAPESP grant 05/56555-4, CNPq/BMBF grant 690144/01-6, and a Marie Curie International Incoming Fellowship within the 7th European Community Framework Programme. This article is a contribution to Imperial College's Grand Challenges in Ecosystems and the Environment initiative. The data reported in this paper can be obtained by contacting the corresponding author, and the R code used in analyses is provided in the supplementary materials. C.B.-L., R.P., L.R.T., A.A.B., R.T.B., T.H.C., M.D., A.T.I., and A.C.M. carried out the data collection; C.B.-L., L.R.T., and W.D.P. analyzed the data; C.B.-L., R.P., L.R.T., W.D.P., and J.P.M. wrote the paper.

SUPPLEMENTARY MATERIALS

www.sciencemag.org/content/345/6200/1041/suppl/DC1
Materials and Methods
Figs. S1 to S3
Tables S1 and S2
References (*27*–*40*)
Appendix

7 May 2014; accepted 23 July 2014
10.1126/science.1255768

PALEOCEANOGRAPHY

Holocene history of ENSO variance and asymmetry in the eastern tropical Pacific

Matthieu Carré,[1]* Julian P. Sachs,[2] Sara Purca,[3] Andrew J. Schauer,[4] Pascale Braconnot,[5] Rommel Angeles Falcón,[6] Michèle Julien,[7] Danièle Lavallée[8]

Understanding the response of the El Niño–Southern Oscillation (ENSO) to global warming requires quantitative data on ENSO under different climate regimes. Here, we present a reconstruction of ENSO in the eastern tropical Pacific spanning the past 10,000 years derived from oxygen isotopes in fossil mollusk shells from Peru. We found that ENSO variance was close to the modern level in the early Holocene and severely damped ~4000 to 5000 years ago. In addition, ENSO variability was skewed toward cold events along coastal Peru 6700 to 7500 years ago owing to a shift of warm anomalies toward the Central Pacific. The modern ENSO regime was established ~3000 to 4500 years ago. We conclude that ENSO was sensitive to changes in climate boundary conditions during the Holocene, including but not limited to insolation.

The El Niño–Southern Oscillation (ENSO) represents the largest natural perturbation to the global climate on an interannual time scale, affecting ecosystems and economies globally. Predicting how the amplitude and spatial pattern of ENSO will change in response to evolving radiative forcing from the buildup of greenhouse gases in the atmosphere is a scientific challenge (*1*) that requires knowledge of the character of ENSO under a range of climate boundary conditions as observed during the Holocene epoch.

A central paradigm of ENSO–mean state studies for the past decade has been that changes in insolation resulting from cyclical changes in Earth's orbital geometry exert a strong control on ENSO (*2*–*4*). This hypothesis was recently called into question by a series of coral oxygen isotope ($\delta^{18}O$) records from the Line Islands in the central Pacific showing large variability in the amplitude of ENSO variance over the past 7000 years, but no significant difference between the middle Holocene and the past millennium (*5*). Furthermore, no reconstructions of ENSO have yet been able to document changes in the spatial pattern of ENSO that are now recognized to account for an important component of its global teleconnections (*6*). We used a technique based on $\delta^{18}O$ variations in fossil mollusk shells from the coast of Peru (*7*) to quantify changes in the amplitude and spatial pattern of ENSO through the Holocene.

We reconstructed the distribution of ENSO-related sea surface temperature (SST) anomalies in the eastern tropical Pacific from monthly records of $\delta^{18}O$ values in fossil *Mesodesma donacium* shells on the coast of Peru. *M. donacium* is a fast-growing aragonitic bivalve that inhabits the surf zone of sandy beaches. Well-preserved shells were collected from radiocarbon-dated intervals at seven coastal archaeological sites (*8*) between 11.7 °S and 18.1 °S (Fig. 1, fig. S1, and table S1). *M. donacium* has been gathered and consumed by fishermen for more than 10,000 years (*9*), resulting in anthropogenic shell mounds up to 10 m in height along the Peruvian coastal desert (figs. S2 to S8). Shells were generally perfectly preserved owing to extremely arid conditions, ensuring the fidelity of $\delta^{18}O$ values (figs. S9 and S10) (*8*). Previous calibration work has demonstrated that *M. donacium* shells faithfully record 1 to 4 years of SST variability with ~1 month resolution (Fig. 1C), yielding quantitative estimates of the seasonal SST range (ΔT) in the coastal water (*10*). By analyzing a random sample of shells from a single depth interval that encompasses several decades or centuries of accumulation, the mean, variance, and skewness of coastal ΔT is obtained, as validated with modern specimens (*7*). A rigorous evaluation of the standard error for the mean, variance, and skewness of coastal ΔT was conducted with a series of pseudo-proxy Monte Carlo simulations that took into consideration the uncertainties associated with isotopic analyses, sampling within climate variability, mesoscale spatial variability, and shell growth, enabling the statistical significance of results to be ascertained (*11*).

Peruvian surf clams share similarities with corals as paleoclimate proxies in that the seasonality of SST can be resolved (*5*), and with individual foraminifera (*12*), because a sample of several specimens is required to statistically extract ENSO characteristics. *M. donacium* shells record ENSO variance resulting from La Niña anomalies and moderate El Niño anomalies but do not record extreme El Niño events. When coastal Peru SSTs warm dramatically (maximum anomaly of 7.7°C in January 1998 in Callao), mass mortality of *M. donacium* occurs. Nevertheless, the distribution of ΔT from a sample of modern shells, though truncated, accurately captures the positively skewed distribution of ENSO in the eastern Pacific (*7*). Our composite Holocene record from 180 mollusk shells and seven archaeological sites thus yields a quantitative reconstruction of mean annual SST, mean ΔT, as well as ENSO variance and skewness for coastal Peru. Because the variance of coastal Peruvian ΔT is highly correlated with the variance of SST anomalies in the Niño1+2 region [correlation coefficient (r) = 0.85], var(ΔT) in Peru can be used as a reliable indicator of ENSO variance in the eastern tropical Pacific (*7*).

Mean annual SST was significantly lower 4.5 thousand years ago (ka) to 9.6 ka than today, especially in southern Peru, where SSTs were ~3°C cooler (Fig. 2A). These cooler conditions imply an increase in the intensity of coastal upwelling (*13*, *14*). Although highly variable, the seasonal range of SST (ΔT) was significantly reduced compared with the late 20th century during most of the Holocene, with reductions up to ~30% (equivalent to ~1.1°C) 0.5, 4.7, 8.5, and

[1]UM2-CNRS–Institut pour la Recherche et le Développement (IRD), Institut des Sciences de l'Evolution de Montpellier, UMR 5554, Place Eugène Bataillon, 34095 Montpellier, France. [2]School of Oceanography, University of Washington, Post Office Box 355351, Seattle, WA 98195, USA. [3]Instituto del Mar del Perú (IMARPE), Esquina Gamarra y general Valle S/N, Callao, Perú. [4]Department of Earth and Space Sciences, University of Washington, Post Office Box 351310, Seattle, WA 98195, USA. [5]Institut Pierre-Simon Laplace/Laboratoire des Sciences du Climat et de l'Environnement, unité mixte CEA-CNRS–Université de Versailles Saint-Quentin-en-Yvelines, Orme des merisiers, Bâtiment 712, 91191 Gif sur Yvette, France. [6]Ministerio de Cultura, Museo de sitio de Pachacamac, Lurín, Lima, Perú. [7]Archéologies et Sciences de l'Antiquité, UMR 7041, Maison René Ginouvès, 21 Allée de l'Université, 92023 Nanterre, France. [8]Archéologie des Amériques, UMR 8096, Maison René Ginouvès, 21 Allée de l'Université, 92023 Nanterre, France.
*Corresponding author. E-mail: matthieu.carre@univ-montp2.fr